

# Multilayered BN Coatings Processed by a Continuous LPCVD Treatment onto Hi-Nicalon Fibers

S. Jacques, H. Vincent, C. Vincent, A. Lopez-Marure, and J. Bouix

Laboratoire des Multimatériaux et Interfaces, UMR 5615 University of Lyon 1/CNRS, 43 boulevard du 11 Novembre 1918, F-69622 Villeurbanne Cedex, France

Received January 24, 2001; in revised form September 5, 2001; accepted September 7, 2001

IN HONOR OF PROFESSOR PAUL HAGENMULLER ON THE OCCASION OF HIS 80TH BIRTHDAY

**Boron nitride coatings were deposited onto SiC fibers by means of continuous low-pressure chemical vapor deposition (LPCVD) treatment from BF<sub>3</sub>/NH<sub>3</sub> mixtures. This process lies in unrolling the fiber in the reactor axis. The relationships between the processing parameters and the structure of the BN deposits are presented. Thanks to a temperature gradient present in the reactor, multilayered BN films can be performed by stacking successive isotropic and anisotropic sublayers. Tensile tests show that when the temperature profile is well adapted, the SiC fibers are not damaged by the LPCVD treatment.** © 2001

Elsevier Science

**Key Words:** LPCVD; boron nitride; structural anisotropy; thin layer; fiber; temperature gradient.

## INTRODUCTION

SiC/SiC ceramic matrix composites (CMCs) have been developed for thermomechanical applications. To achieve good toughness, the addition of a thin film (thickness < 0.5 μm) of a compliant material called “interphase” between the fiber and the matrix is required (1). Hence, the interphase allows the fiber/matrix coupling to be optimized. Owing to its structural anisotropy, pyrolytic turbostratic boron nitride processed by low-pressure chemical vapor deposition (LPCVD) can play such a role (2).

On one hand, Hinke *et al.* have shown that BN films can be prepared continuously onto carbon fibers by a continuous CVD process using the reaction of BCl<sub>3</sub> with NH<sub>3</sub> at temperatures ranging from 700 to 1000°C (3). But with these conditions, BN is expected to be poorly organized and remains isotropic. Nevertheless, we have demonstrated before that the use of such a continuous process in which the fiber is unrolled in the reactor axis allows significant length of fibers to be treated (4).

On the other hand, it is possible to obtain a highly crystallized BN by CVD from the BF<sub>3</sub>-NH<sub>3</sub> gaseous system, but this processing requires the SiC fiber to be

protected from a chemical attack with an isotropic BN precoating obtained with less aggressive conditions (5,6). Thus, in the case of a classical static isothermal CVD, such a multilayered BN film must be infiltrated by following several separate stages (i.e., changing the boron precursor gas and CVD parameters during the experiment, etc.).

The aim of the present paper was to coat SiC fibers with BN films containing at least one anisotropic sublayer by using a one-step continuous dynamic LPCVD process from the BF<sub>3</sub>-NH<sub>3</sub> system without damaging the SiC fiber.

## EXPERIMENTAL

### Processing

The BN coatings were processed by LPCVD. They were deposited around each filament of a Hi-Nicalon fiber tow (from Nippon Carbon, Japan). The reactor was a hot wall furnace: a graphite susceptor (length: 35 cm) placed inside a silica tube (inner diameter: 24 mm) was heated by induction. For continuous dynamic study, the fiber tow was unwound from the first spool through the susceptor. The reactor outlet winding around a second spool controlled the fiber travelling rate  $r$  (Fig. 1). For static study, the fiber tow was motionless ( $r = 0$ ). BF<sub>3</sub> and NH<sub>3</sub> were the BN gaseous precursors, and argon was used as the gas vector but also to dilute the reactive species. BF<sub>3</sub> and NH<sub>3</sub> were separately introduced into a cold area of the reactor and mixed near the entrance of the hot susceptor. The total gas flow rate  $Q$  was 100 cm<sup>3</sup> min<sup>-1</sup> and the ratio  $Q_{\text{Ar}}/(Q_{\text{BF}_3} + Q_{\text{NH}_3})$  was 0.1. The initial gas composition was determined by  $\alpha = Q_{\text{NH}_3}/Q_{\text{BF}_3}$ . The susceptor temperature was measured by means of an optic pyrometer.

### Characterization

After treatment, the samples were broken and the fracture surfaces of the BN deposits were observed with a scanning electron microscope (SEM) (Hitachi S800).

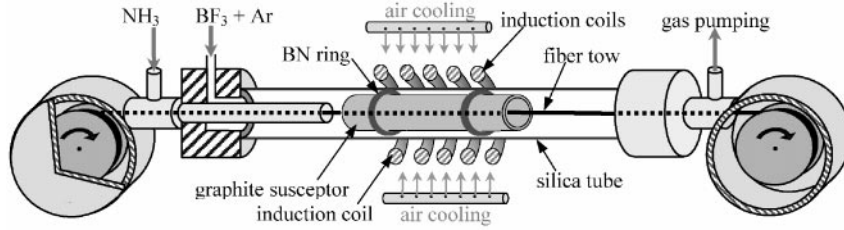


FIG. 1. Apparatus used for continuous BN processing (schematics).

Structural measurements were performed by two complementary methods: X-ray diffraction (XRD: Philips PW 3710,  $\lambda_{\text{Cu}} = 0.15418$  nm) and Raman spectroscopy (Jobin-Yvon, Ramanor,  $\lambda = 514.5$  nm). In theory, coherent length  $L_c$  and  $L_a$  can be respectively deduced from the full width at half-maximum (fwhm) of the 002 ( $2\theta = 26.7^\circ$ ) and 100 ( $2\theta = 41.6^\circ$ ) diffraction bands by the Scherrer equation:

$$L = \frac{k\lambda}{\text{fwhm} \cos \theta}.$$

In practice, only the 002 band is intense and well defined enough for this calculation ( $k = 1.84$ ). The 100 band analysis is possible ( $k = 0.9$ ) but a deconvolution of the superimposed 100 and 101 bands is required. Raman spectroscopy allows a better estimation of the average graphitic plan length from the  $1367\text{-cm}^{-1}$  band analysis. The fwhm of this band is proportional to  $1/L_a$  (7).

The chemical composition of the BN deposits was determined by X-ray photoelectron spectroscopy (XPS: Hewlett-Packard 5950A) using a focused monochromatic  $\text{AlK}\alpha$  radiation (1486.6 eV).

Tensile tests were performed at room temperature on coated fibers (separated at random from the treated tow) and uncoated fibers (as a reference) with an MTS-Adamel DY-22 machine (Ivry sur Seine, France) equipped with a 5 N load cell. The crosshead speed was 0.1 mm/min. In each case, a batch of about 50 monofilaments was tested

with a 20-mm gauge length. The characteristic fiber failure stress was determined by using the Weibull statistics with an associated probability of failure equal to 0.632 (8,9).

## RESULTS AND DISCUSSION

### Static LPCVD Process Study

The influence of temperature, total pressure, and initial gas-phase composition  $\alpha$  was first studied without fiber displacement, using isothermal and isobar conditions. With these “static” treatments (about 1-h duration), the coatings were thick enough to determine their morphology or apparent texture by means of a simple SEM observation. As the temperature was not uniform along the whole susceptor length, the coated fiber was always extracted from the same place located in the hottest reactor area. This qualitative observation evidences the occurrence of three possible textures for the BN coatings. They are referred to as smooth isotropic ( $I_s$ ), rough isotropic ( $I_r$ ), and anisotropic ( $A$ ). The texture  $I_s$  corresponds to a flat aspect of the fracture surface (Fig. 2a) while the  $I_r$  fracture surface seems to be rougher but still homogeneous and without preferential grain orientation or distribution (Fig. 2b). The BN coatings with texture  $A$  clearly exhibit a laminated fracture surface (Fig. 2c).

Obviously, the formation of each texture depends on the pressure, the temperature, and the initial gas-phase composition. Thanks to numerous experimental runs, texture diagrams could be established where each domain gives

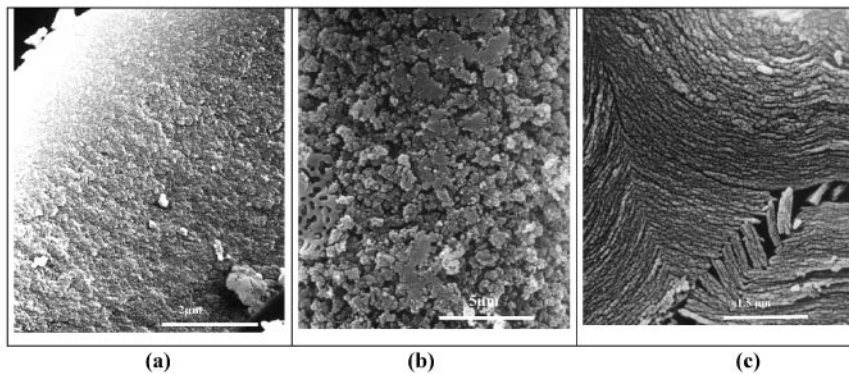


FIG. 2. Different textures for the BN coatings: (a) smooth isotropic ( $I_s$ ); (b) rough isotropic ( $I_r$ ); (c) anisotropic ( $A$ ).

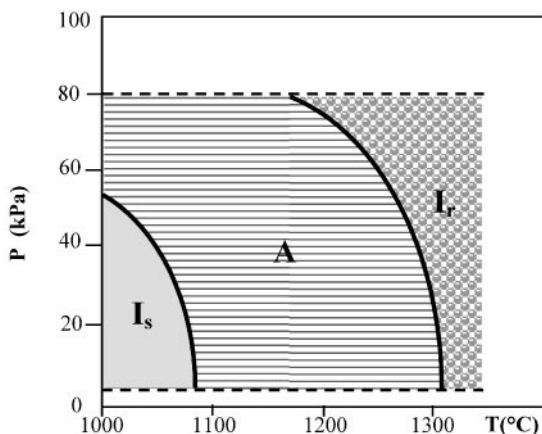


FIG. 3. Pressure versus temperature texture diagram ( $\alpha = 2$ ).

relationships between a given texture and CVD processing conditions. The transition from one texture domain to another is comparatively sharp.

*Influence of Total Pressure and Temperature*

A first diagram is reported in Fig. 3 for  $\alpha = 2$ . Domain  $I_s$  is restricted to a low temperature ( $< 1070^\circ\text{C}$ ) and low-pressure scale ( $< 50\text{ kPa}$ ). Domain  $A$  appears for intermediate temperatures and extends over a large range of pressure.

As a general rule, lamellae are more pronounced as the pressure increases. This feature is confirmed by XRD and Raman spectroscopy, which show an increase of the crystallite size with the pressure increasing (Fig. 4). Finally, domain  $I_r$  appears at high temperature.

A second texture diagram is reported in Fig. 5 for  $\alpha = 0.5$ , i.e., for a higher  $\text{BF}_3$  content in the initial gas phase. In that case, domain  $A$  is very narrow at low pressure and widens out when pressure increases. For instance, the deposit is laminated for  $P = 5\text{ kPa}$  and  $1050 < T < 1150^\circ\text{C}$  and

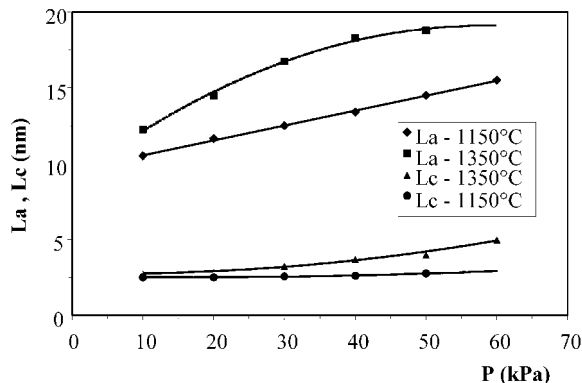


FIG. 4.  $L_a$  and  $L_c$  (XRD) versus pressure ( $\alpha = 0.5$ ,  $T = 1150$  and  $1350^\circ\text{C}$ ).

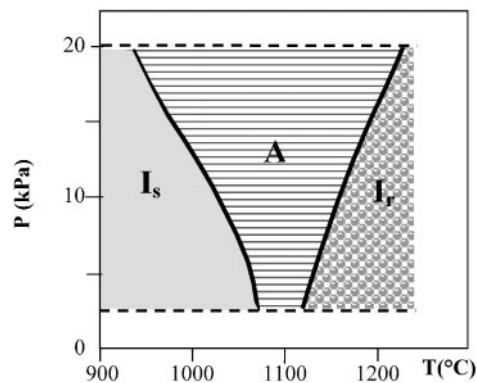


FIG. 5. Pressure versus temperature texture diagram ( $\alpha = 0.5$ ).

for  $P = 20\text{ kPa}$  and  $950 < T < 1250^\circ\text{C}$ . Thus, with  $P = 20\text{ kPa}$ , which is a low enough pressure for a good infiltration of a fiber tow, an anisotropic BN coating can be obtained at almost any temperature. So pressure was maintained at  $20\text{ kPa}$  for the following study.

*Influence of alpha Composition and Temperature*

This study was restricted at  $\alpha > 0.5$ . Below this limit, the gas is too aggressive toward the Hi-Nicalon fiber. Fig. 6 shows that domain  $A$  temperature range decreases when the gas mixture becomes impoverished of  $\text{BF}_3$ . Thus, the coating is anisotropic for  $\alpha = 0.5$  and  $900 < T < 1300^\circ\text{C}$ , for  $\alpha = 2$  and  $1020 < T < 1250^\circ\text{C}$ , and for  $\alpha = 5$  and  $1120 < T < 1200^\circ\text{C}$ . For  $\alpha > 6$ , only an isotropic deposit is observed at any temperature.

*BN Growth Mechanism*

Quantitative XPS analyses revealed that every deposit is made of stoichiometric BN. The equivalence ratio B/N remains comparatively constant; it ranges from 0.98 for  $\alpha = 1$  to 1.02 for  $\alpha = 0.5$ . Thus, the different textures are not

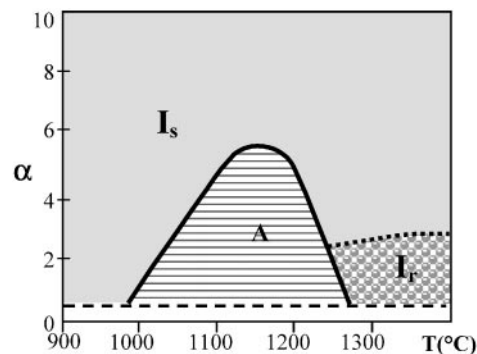


FIG. 6.  $\alpha$  versus temperature texture diagram ( $P = 20\text{ kPa}$ ).



FIG. 7. Deposit processed with homogeneous nucleation ( $T > 1300^{\circ}\text{C}$ ).

connected with composition variation. A  $\text{BF}_3$ -rich mixture (low  $\alpha$ ) is favorable to an anisotropic BN processing. This feature can be explained by the trigonal planar geometry (with bond angles of  $120^{\circ}$ ) of a  $\text{BF}_3$  molecule that foreshadows the  $\text{B}_3\text{N}_3$  hexagonal shape of boron nitride. In contrast, the pyramidal shape of ammonia is detrimental to

BN structural organization. Consequently, the BN deposit becomes isotropic for high  $\alpha$  values.

A previous kinetic study carried out by Prouhet *et al.* on CVD BN growth can explain the sharp transition from one texture to another (10). The conditions of this work were similar to the present study. Prouhet *et al.* reported that the BN growth rate is governed by different mechanisms depending on pressure and temperature processing. For a given pressure, below a pivot temperature, the BN growth is governed by a surface reaction mechanism, and above, it switches to a diffusion mechanism. From a comparison between both studies, it appears that the former mechanism at low temperature yields texture  $I_s$ , while the latter at higher temperature yields texture  $A$ . An interpretation of the third texture  $I_r$ , obtained at high temperature ( $> 1200\text{--}1300^{\circ}\text{C}$ ) is more delicate. The deposit surface roughness (with sometimes outgrowths) could be explained by a homogeneous nucleation. Figure 7 illustrates a pronounced case.

#### Transient Mechanism Treatment

Texture diagrams reveal that a slight variation of one CVD process parameter ( $\alpha$ ,  $T$ , or  $P$ ) can result in a deposit texture transition. This feature was first illustrated with an experiment in which the pressure has been continuously increased from 0 to 20 kPa for 40 min and then maintained constant for 30 min at  $1200^{\circ}\text{C}$  with  $\alpha = 0.5$ . SEM observation of the deposit (Fig. 8a) shows that it is made of two layers: the first one near the fiber is isotropic  $I_s$  and corresponds to low pressures and the second one is clearly anisotropic with lamellae orientated parallel to the fiber surface. A second experiment was carried out at 20 kPa with  $\alpha = 0.5$

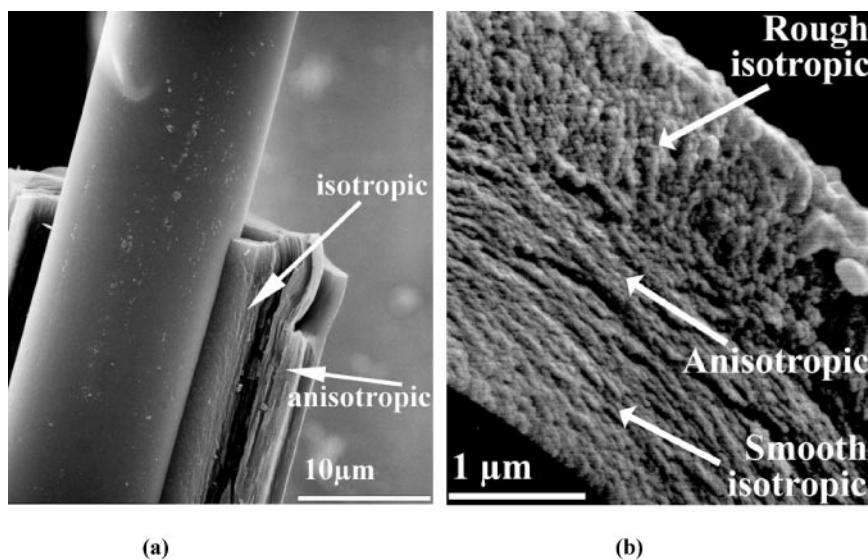


FIG. 8. Multilayered coating: with increasing pressure (a); with increasing temperature (b).

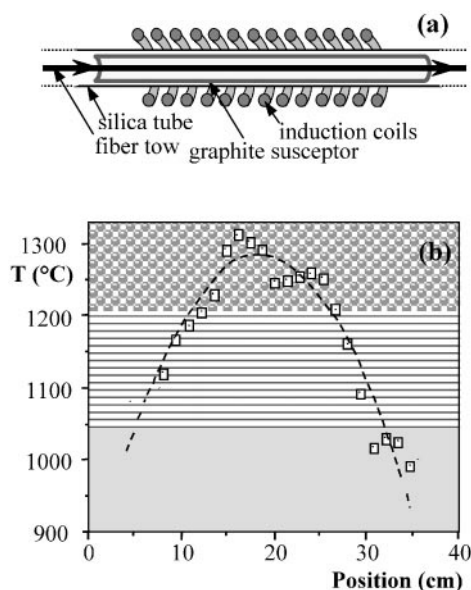


FIG. 9. Schematics of the reactor (a) and temperature profile (b) measured along the susceptor (—□—).

and temperature increasing continuously from 950 to 1300°C. SEM observation confirms the occurrence of a first isotropic layer  $I_s$ , followed by a second anisotropic layer  $A$  and a third rough layer  $I_r$  (Fig. 8b).

#### Continuous Dynamic LPCVD Process Study

The aim of the present study was to perform a continuous dynamic treatment, i.e., with a fiber tow displacement

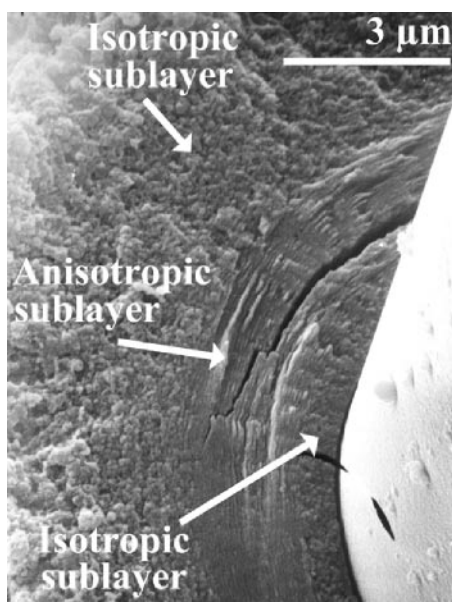


FIG. 10. BN coating with three sublayers ( $P = 20$  kPa,  $T_{\max} = 1300^\circ\text{C}$ ,  $\alpha = 2$ ).

through the susceptor. During such a treatment,  $\alpha$  and  $P$  remain constant but the fiber undergoes a temperature profile while traveling: the temperature continuously increases from a “cold” area at the entrance to a hot area at the center ( $T_{\max}$ ) and finally decreases at the outlet of the susceptor. The temperature profile measured along the susceptor is given in Fig. 9.

With  $\alpha = 2$  and  $P = 20$  kPa, according to texture diagrams, the BN coating should be made of five sublayers with the following expected theoretical sequence:  $I_s/A/I_r/A/I_s$ . By using a low displacement rate ( $r = 0.5$  m h<sup>-1</sup>), we can observe that the experimental coating is made of only three sublayers (Fig. 10)  $I_s/A/I_r$ . The absence of the last two sublayers can be due to a sharp decrease of the reactive gaseous species content at the outlet of the reactor.

With high displacement rates ( $r \geq 3$  m h<sup>-1</sup>), the BN deposits are thinner ( $< 0.5$  μm) and difficult to observe by SEM. Such thicknesses are compatible with interphases of CMCs but in these conditions the coated fiber failure stresses are significantly lowered ( $\sigma_F < 2000$  MPa) compared with the initial value of the nontreated Hi-Nicalon fiber ( $\sigma_F \approx 3000$  MPa). This feature evidences that the SiC fiber does not stay long enough in the low-temperature area and consequently the first isotropic layer cannot protect it.

To overcome this phenomenon, the initial susceptor temperature profile was modified: the total “cold” temperature area is increased thanks to a variable pitch of induction heating coil turns (Fig. 11). Thus, the reactor contained three distinct hot areas with respectively a “low” temperature ( $< 1100^\circ\text{C}$ ), a medium maximum temperature ( $\sim 1150^\circ\text{C}$ ), and a high one ( $\sim 1250^\circ\text{C}$ ).

The idea was to favor the isotropic coating growth that protects the fiber before aggressive coating conditions. Such

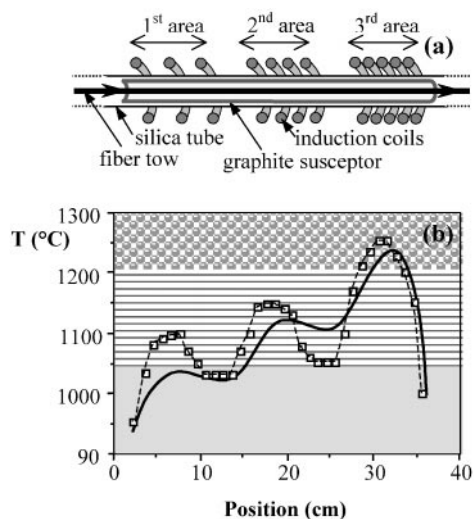


FIG. 11. Schematics of the susceptor with modified induction heating (a) and temperature profile (b) measured along the susceptor (—□—) and actually followed by the fiber tow at  $r = 0.5$  m h<sup>-1</sup> (—).

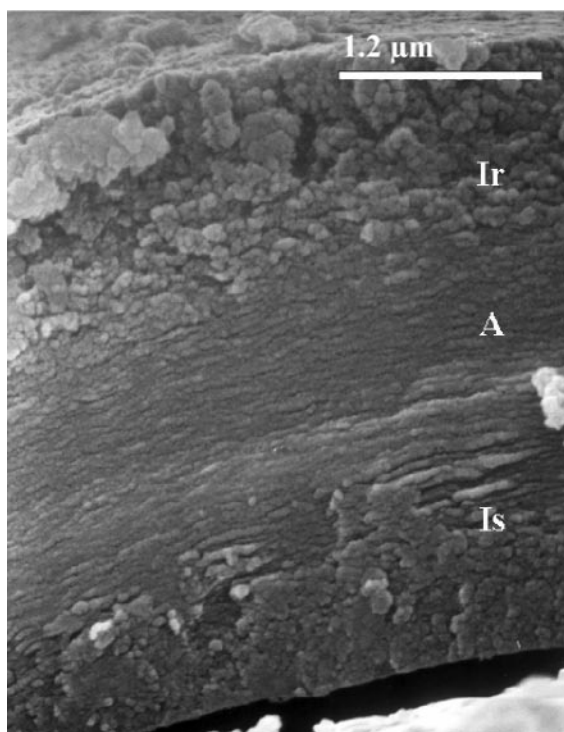


FIG. 12. BN coating with three sublayers.

a temperature profile should promote pronounced transitions between each sublayer. At the outcome of the susceptor, the temperature gradient is very high and, consequently, the rapid resulting cooling should prevent an external  $I_s$  layer formation. Hence, the last sublayer obtained in the hottest area should be rough ( $I_r$ ) and favorable to good further adhesion of a SiC matrix. Still with  $\alpha = 2$  and  $P = 20$  kPa, if the fiber tow follows exactly the measured temperature profile, the expected BN coating should contain the following sequence of sublayers:  $I_s/A/I_s/A/I_r$ . Actually, with  $r = 0.5$  m h<sup>-1</sup> the third expected sublayer  $I_s$  is not observed (Fig. 12).

This discrepancy is certainly due to a different temperature profile followed by the fiber tow: because of the displacement, fiber heating and cooling are slightly delayed along the susceptor (Fig. 11). It is worth noting that the growth rate of BN depends on temperature and, conse-

quently, sublayer thickness does not proportionally correspond to texture domain lengths shown by the schematics.

With a high displacement rate ( $r = 3$  m h<sup>-1</sup>), the total BN deposit thickness is about 0.8 μm and tensile tests do not evidence a significant decrease of the fiber failure stress. The study of such BN coatings as interphases in SiC/SiC composites is reported elsewhere (11).

## CONCLUSION

Thin BN layers with a lamellar structure could be deposited from  $BF_3$  and  $NH_3$  gaseous species onto fibers that were traveling continuously inside a LPCVD reactor. The structural anisotropy can be obtained at 20 kPa above 1200°C. These conditions are aggressive toward the fiber. Nevertheless, the occurrence of a temperature gradient along the susceptor heated by induction enables in one step a multilayered coating with different textures to be processed. If the first cold area located at the entrance of the susceptor is extended enough, the first BN sublayer is isotropic and protects the Hi-Nicalon fiber from the aggressive gaseous mixture at high temperature. In these conditions, the mechanical properties of the treated and nontreated fibers are similar. The use of such BN thin coatings as interphases in ceramic matrix composites can be considered.

## REFERENCES

1. A. G. Evans and F. W. Zok, *J. Mater. Sci.* **29**, 3857 (1994).
2. J. P. Singh, D. Singh, and R. A. Lowden, *Ceram. Eng. Sci. Proc.* **15**(4), 456 (1994).
3. S. Hinke, S. Stöckel, and G. Marx, *Fresenius J. Anal. Chem.* **349**, 181 (1994).
4. J. Bouix, C. Vincent, H. Vincent, and R. Favre, *Mater. Res. Soc. Symp. Proc.* **168**, 305 (1990).
5. F. Rebillat, A. Guette, L. Espitalier, C. Debieuvre, and R. Naslain, *J. Eur. Ceram. Soc.* **18**, 1809 (1998).
6. F. Rebillat, A. Guette, and C. R. Brosse, *Acta Mater.* **47**(5), 1685 (1999).
7. R. J. Neamanich, S. A. Solin, and R. M. Martin, *Phys. Rev.* **23**(12), 6348 (1981).
8. B. Bergman, *J. Mater. Sci. Lett.* **5**, 611 (1986).
9. S. N. Patankar, *J. Mater. Sci. Lett.* **10**, 1176 (1991).
10. S. Prouhet, F. Langlais, A. Guette, and R. Naslain, *J. Solid State Inorg. Chem.* **30**(10), 953 (1993).
11. S. Jacques, A. Lopez-Marure, C. Vincent, H. Vincent, and J. Bouix, *J. Eur. Ceram. Soc.* **20**(12), 1929 (2000).